Chalcogenide Letters Vol. 14, No. 8, August 2017, p. 321 - 329

ANNEALING TREATMENTS AND CHARACTERIZATION OF PbS-CdO CORE-SHELL THIN FILM FOR SOLAR ENERGY APPLICATIONS

C. AUGUSTINE[a,b*], M. N. NNABUCHI[a], F. N. C. ANYAEGBUNAM[b], C. U. UWA[c]
[a]*Department of Industrial Physics, Ebonyi State University, Abakaliki, Nigeria*
[b] *Department of Physics, Federal University Ndufu Alike Ikwo, Ebonyi State, Nigeria*
[c]*Department of Biological Science, Federal University Ndufu-Alike Ikwo, Ebonyi State, Nigeria*

Using chemical bath deposition technique, five samples of heterojunction core-shell thin films of PbS/CdO were deposited on plane glass substrates at bath temperature of 353K. Two out of the five thin film samples were subjected to 473K and 673K annealing temperatures in order to investigate the effect of thermal annealing on the properties of interest while one sample was left as control. XRD studies showed that the double layer components were polycrystalline with sharp and dominant peaks. Peak broadening was observed in the recorded diffraction patterns of the polycrystalline thin films. Four point probe analysis showed that the conductivity varied proportionally with temperature indicating that the films are semiconductors. UV studies reveals that the transmittances of the films were significantly modified by heat treatments. In particular, the transmittance was lowest for the film annealed at 673K. The band gap was observed to decrease with an increase in annealing temperature, with values in the range (1.25 - 1.75eV) suitable for solar photovoltaic and thermal applications.

(Received June 12, 2017; Accepted August 11, 2017)

Keywords: Annealing, Bandgap, Chemical Bath, Conductivity, Temperature

1. Introduction

Energy is the motive force behind the sustained technological development of any nation and Nigeria is blessed with reasonably high quantities of various energy resources. These include the non-renewables such as crude oil, natural gas, coal and uranium and the renewables such as biomass, solar, wind and hydro energy. At present, the dominant energy source used in Nigeria is oil and its derivatives, accounting for over 75% of the total energy consumption except in the rural areas where biomass in the form of fuel wood dominates.

The environmental consequences of harnessing these non-renewable energy sources are assuming alarming proportions. Therefore, Economic and environmental reasons are making us to shift emphasis to the renewable energy resources. One of the most viable options particularly in Nigeria is the abundant solar energy falling on the surface of the earth. Nigeria is blessed with enormous solar radiation that can be harnessed; solar radiation intensity varies from 7.0kwh/m^2 at the extreme north to 3.5kwh/m^2 in the extreme south. These figures are sufficient for thermal and photovoltaic applications [1].

Photovoltaic is the most useful way of utilizing solar energy by directly converting it into electricity. The first generation of solar cells were made from semiconductor materials like silicon. However, the high cost of processing silicon materials has limited large production of solar cells for commercial purposes. The goal of bringing photovoltaic cells down to the cost of conventional electricity may only be achieved if they are made of polycrystalline thin films as well as non-

* Corresponding author: emmyaustine2003@yahoo.com

silicon compounds that are relatively inexpensive and readily available. Thin film approach of producing solar cells reduces cost by using small amount of material and inexpensive processing.

In recent years, the development of core-shell structured materials have been receiving extensive attention because of their various applications such as coatings, solar cells and photocatalysis [2]. The shell can alter the charge, functionality, and reactivity of surface, or improve the stability and dispersive ability. Furthermore, catalytic, optical, or magnetic functions can be imparted to the core particles by the shell material. In general, the synthesis of core/shell structured material has the goal of obtaining a new composite material having synergetic or complementary behaviours between the core and shell materials [2].

There are many studies on the synthesis of core-shell thin film materials. The effects of thermal annealing on the optical and band gap of TiO_2/Fe_2O_3, TiO_2/CoO and TiO_2/CuO core-shell thin films have been reported [3-5]. Particle size analysis for different substrate of ZnS/ZnO core-shell has been studied [6]. Core-shell thin films of TiO_2 /Fe_2O_3, TiO_2/CuO, ZnO/PbS, ZnO/CuS, CdS/PbS, TiO_2/PbS have been studied for various solar energy applications [7-12].

In this study, we report the synthesis of PbS/CdO thin film via simple and inexpensive chemical both deposition technique. We also present the effect of post deposition annealing on the as-deposited film at temperature of 473K and 673K.

2. Theory

The use of thin films in optical applications require accurate knowledge of the optical constants over a wide wavelength range [13]. Most spectrophotometer give the absorbance data from which transmittance, absorption coefficient and other optical constants were determined. The relationship between the absorbance, A and transmittance, T is thus:

$$\mathrm{T} = 10^{-\mathrm{A}} \tag{1}$$

The absorption coefficient, α of thin films can be expressed in terms of absorbance, A and thickness, t as [14].

$$\alpha = \frac{2.3026 \times \mathrm{A}}{t} \tag{2}$$

This absorption coefficient, α is related to the energy gap, E_g of a semiconductor [15]:

$$(\alpha h\nu)^2 = \mathrm{A}\left(h\nu - \mathrm{E}_g\right)^n \tag{3}$$

Where A is a constant, hv is the photon energy, α is the absorption coefficient and n is an index that characterises the nature of the transition. For n = 1/2, the transition is generally accepted to be direct. Hence a linear graph of $(\alpha h\nu)^2$ versus hv will show E_g as intercept on hv axis. However, the usual difficulty in applying this concept to polycrystalline thin films with nanometre scale crystalline grain is the size distribution of grains and consistent change in the band gap due to quantum confinement effect [16, 17]. Thus the straight line portion may not extend beyond a few tenths of an electron volt and hence value of the band gap could turn out to be very subjective [18].

The change in energy band gap is given by [19]:

$$\Delta E_g = \frac{\frac{\hbar^2\pi^2}{2R^2}\left(\frac{1}{M_e} + \frac{1}{M_h}\right) - \left(1.786e^2\right)}{\varepsilon_r} \tag{4}$$

Where M_e , M_h are the effective masses of electrons in the conduction band and holes in the valence band respectively, E is the static dielectric constant of the material and ΔE_g is the change in the band gap. The first term represents the particle in a-box quantum localization energy and has an inverse square relation $1/R^2$ dependence where R is the particle radius, while the second term represents the Coulomb energy with 1/R dependence. Therefore as R increases due to the increase in the crystalline size associated with temperature annealing, the value of ΔE_g will decrease.

The electrical characterization of thin films can give a clear idea regarding the transport mechanism related to the electrical conduction which gives the value of electrical resistivity, ρ and conductivity, σ of films. The sheet resistant is given by [20].

$$R_s = 4.53 \times \frac{V}{I} \tag{5}$$

Where V is the measured voltage between the two inner probes and I is the current passed through the outer probes. The resistivity was determined from the relation [21]:

$$\rho = R_s \times t \tag{6}$$

Where t is the thickness of the conducting layer while ρ is the resistivity and R_s is the sheet resistance. From the value of ρ, the conductivity σ was determined using the relation [21] :

$$\sigma = \frac{1}{\rho} \tag{7}$$

3. Experimental

The chemical bath for the deposition of PbS-CdO core-shell thin film was done in the following order. First, the core PbS was deposited in a bath composed of 5mls of 0.2M $Pb(NO_3)_2$, 5mls of 1M SC $(NH_2)_2$, 5mls of 1M NaoH and 35mls of distilled water put in that order in 50ml cleaned and dried beaker. Five (5) clean glass slides were then inserted vertically into the solution. The deposition was allowed to proceed at room temperature for 50 minutes after which the substrates coated with dark deposits were removed, washed with distilled water and allowed to dry. The deposition of PbS/CdO was achieved by inserting the substrates coated with PbS deposits into a mixture containing 10mls of 0.2M $CdSO_4$, 10mls of 1M SC $(NH_2)_2$, 2mls of 100% NH_3 and 30mls of distilled water into 50ml beaker. Deposition was allowed to proceed at temperature of 353K for 1 hr. Two out of the five samples of the core-shell thin films deposited were heated (annealed) at temperatures of 473K, and 673K for one hour in an oven. The purpose of annealing is to know the temperature at which the samples can be exposed without damage and also to investigate the effect of temperature on the properties of the film. One of the remaining samples served as the control during characterization. Thermo scientific GENESYS 10S model UV-VIS spectrophotometer on the 300-1000 nm range of light at normal incidence to samples was used to obtain the absorbance data from which transmittance, absorption coefficient and optical parameters were calculated. Structural studies were done with Rigaku Ultima IV X-ray diffractometer equipped with a graphite-monochromated CuK_α radiation source (40KV, 30mA) and four point probe (Keithley model) was used for the electrical characterization of the film samples.

4. Result and discussion

Rutherford backscattering (RBS) was used to determine the elemental composition, depth profile and thickness of the film samples by Proton Induced X-ray Emission (PIXE) scans on the samples from a Tandem Accelerator Model 55DH 1.7MV Pellaton. The RBS analysis of PbS/CdO

for as-deposited, thermally annealed at 473K and 673K are shown figure 1, 2, and 3 respectively. In RBS analysis, film thickness is determined by the width of the peak. The concentration is determined by the intensity or height of the peak. The thickness of the film samples as deciphered by RBS are 2000nm, 1423nm and 974nm for the as-deposited, thermally annealed at 473K and 673K respectively.

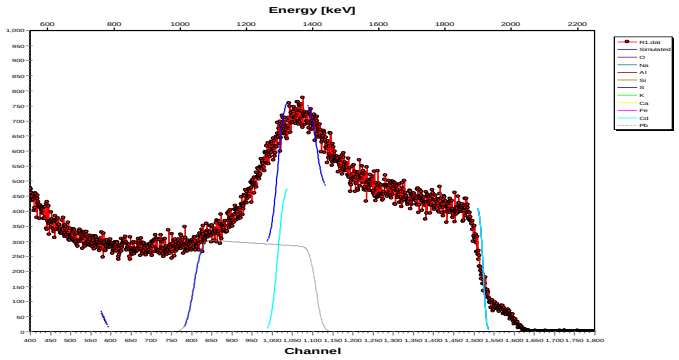

Fig. 1. RBS micro graph of PbS-CdO core-shell thin film as-deposited

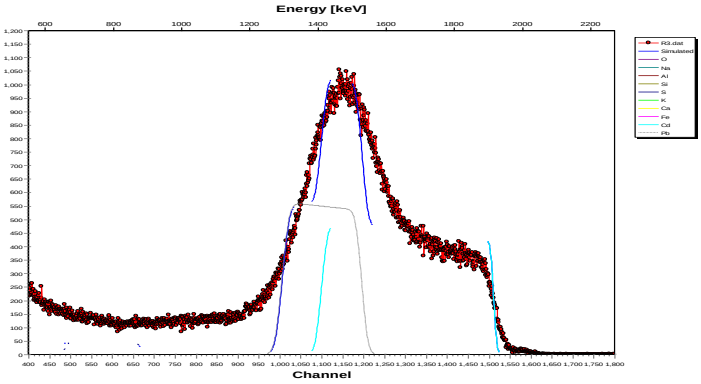

Fig. 2. RBS micro graph of PbS-CdO core-shell thin film at 473K

The chemical status and elemental composition of as-deposited PbS/CdO thin film comprises 11.08% lead (Pb), 70.97% cadmium (Cd), 77.25% sulphur (S) and 29.03% oxygen. The annealed at 473K composed of 18.72% Pb, 91.27% Cd, 79.25% S and 26.27% oxygen. The annealed at 673K consists of 25.61% Pb, 7.73% Cd, 74.35% S and 8.73% oxygen.

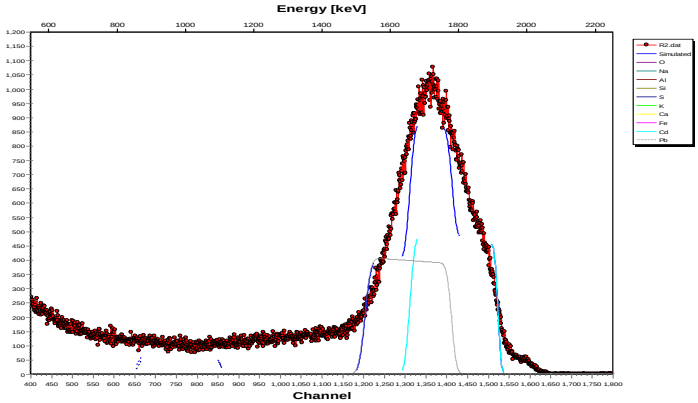

Fig. 3. RBS micro graph of PbS-CdO core-shell thin film at 673K

The XRD diffractograms of PbS-CdO thin films for as-deposited, thermally annealed at 473K and 673K are presented in figures 4, 5 and 6 respectively. Such X-ray spectra display prominent peaks located at the following angular positions: 2θ = [26.00, 30.00, 43.00, 53. 00]. They are related with the reflection peaks of (111), (200), (220), (311) respectively. The diffraction peaks of 2θ = [26^o, 30^o] can be perfectly indexed to Galena PbS displaying the cubic crystalline phase according to reference patterns JCPDS 05-0592. The peak of 2θ values of 43^o is identified to be CdO (JCPDS 00–042-1411). Peak broadening was observed in recorded diffraction patterns of the polycrystalline thin films. The average grain size of the film samples are 68.96nm, 73.49nm and 80.48nm for as deposited, thermally annealed at 473K and 673K respectively.

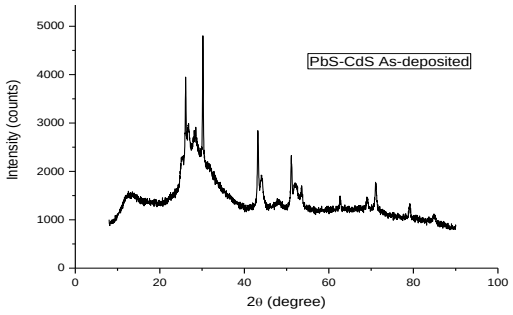

Fig. 4. XRD pattern of PbS-CdO as-deposited

The average grain size of the film samples were calculated using the Debye Scherer's formula [22]

$$D = \frac{0.9\lambda}{\beta \cos\theta} \tag{8}$$

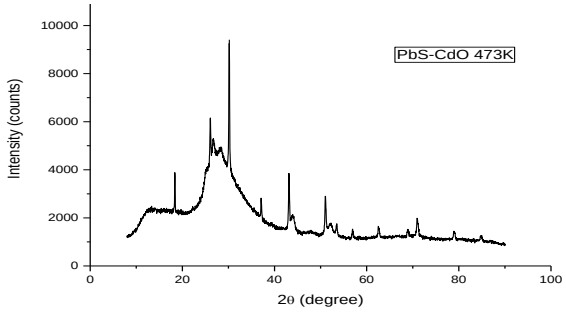

Fig. 5. XRD pattern of PbS-CdO annealed at 473K

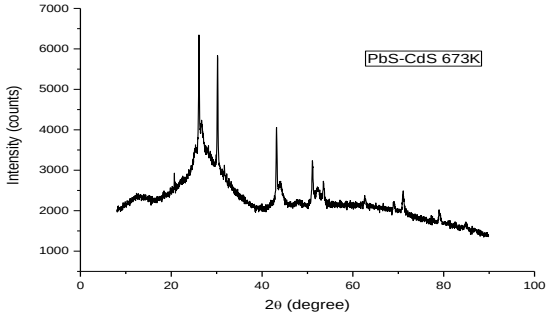

Fig. 6. XRD pattern of PbS-CdO at 673K

The optical absorbance and transmittance are shown in Figs. 7 and 8 respectively. From Fig. 7, it is seen that the strongest absorption peak of the as-deposited appears at 300nm-700nm. Thermally annealed 47K and 673K samples have strongest absorptions at 300nm-750nm and 300nm-850nm respectively. In all these samples, the absorbance is generally high especially in the VU-VIS regions. This characteristics of high absorbance make the film suitable for coating the surface of solar collectors for solar thermal applications. Solar collectors for heating fluids require increasing the reception area of the solar radiation, and/or to increase the absorbance of the surface coating in order to improve thermal efficiency. The spectral distribution in fig. 8 shows that transmittance decreases with annealing temperature exhibiting a maximum for as-deposited sample. This may be a consequence of increase in particle size associated with increase in temperature. This is collaborated by the XRD results which show that the sample annealed at 673K has the highest grain size. The transmittance of thin films can be greatly modified by different deposition parameters. In the literature, the concentration dependent optical behaviour and variation of transmittance caused by different deposition time have been reported [23, 24].

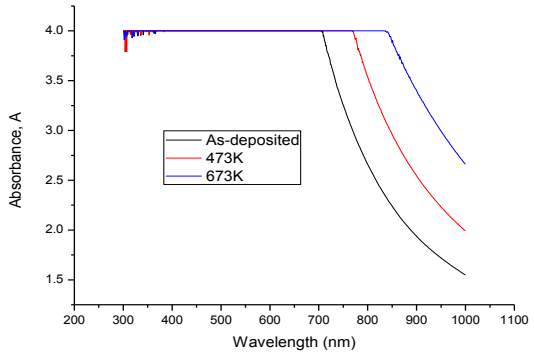

Fig. 7. Optical absorption spectrum of PbS/CdO core-shell at different annealing temperatures

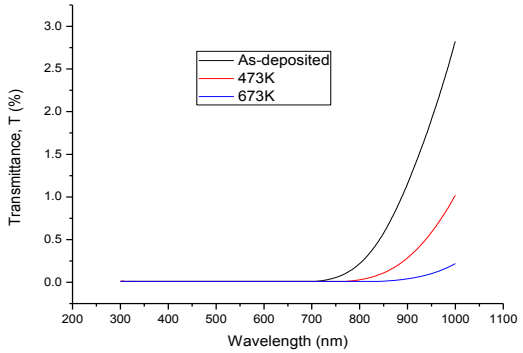

Fig. 8. Optical transmission spectrum of PbS/CdO core-shell at different annealing temperatures

Fig. 9 shows the plots of the absorption coefficient (α) against photon energy (hν) at the different annealing temperatures. The optical absorption coefficient were very high in all the layers. However, the plot of the optical absorption coefficient of the annealed at 673K layer was relatively higher compared to that of the other layers. The high value of the optical absorption coefficient is an indication that the films can be utilized in different optoelectronic devices.

The plot of $(\alpha h\nu)^2$ versus $h\nu$ for the film samples shown is presented in figure 10 and indicates the presence of direct transition. The straight portion is extrapolated to energy axis at α = 0 which gives the band gap energy E_g of the PbS-CdO films as 1.75eV, 1.50eV and 1.25eV for the as-deposited, thermally annealed at 473K and 673K respectively. The value of the energy bandgap of the as-deposited layer was higher, compared to the annealed layers i.e, a clear

indication of bandgap narrowing induced by the post deposition heat treatments. The decrease in the energy bandgap of the heat treated layers was attributed to the increase in grain size and/or related phenomena, caused by the annealing effects [25]. The decrease in energy band gap caused by post deposition heat treatment has been widely reported by other authors [2-4, 26, 27]

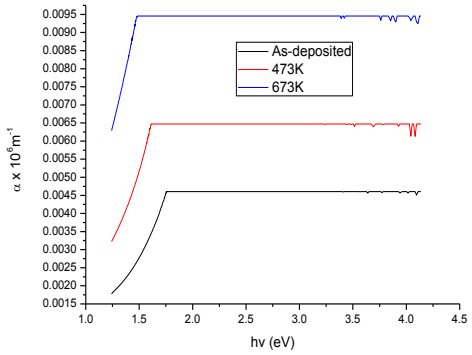

Fig. 9. Absorption coefficient against photon energy plots of PbS/CdO at different annealing temperatures

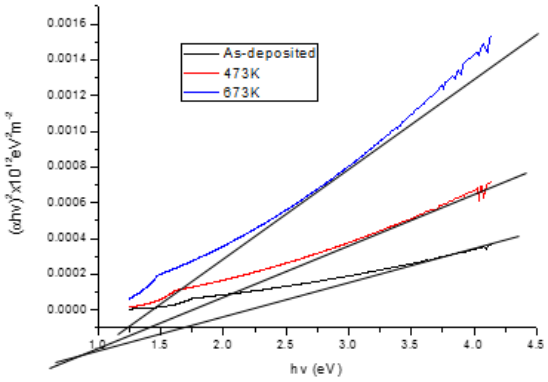

Fig. 10: Plots of $(\alpha hv)^2$ as a function of hv at different annealing temperatures

The decrease in energy band gap is collaborated by the fact that the band gap can be expressed in terms of the effective mass approximation in equation (4). Therefore as R increases due to the increase in the crystalline size associated with temperature annealing, the value of ΔE_g will decrease. Fig. 11 displays the electrical conductivity, σ versus 1000/T curve for as-deposited, thermally annealed 473K and 673K samples. From equation (7), it is obvious that increasing electrical conductivities implies decreasing electrical resistivities, thus the resistivity of the films decreased due to the post deposition heat treatments. The thermally annealed 673K film had the highest electrical conductivity. This may be due to the highest grain size of thermally annealed 673K film. The increase of grain size may be due to the improved crystallanity of 673K film. The growth in grains leads to the reduction of grain boundary scattering which decreases the resistivity for the films and eventually the increase in the conductivity of the films [28].

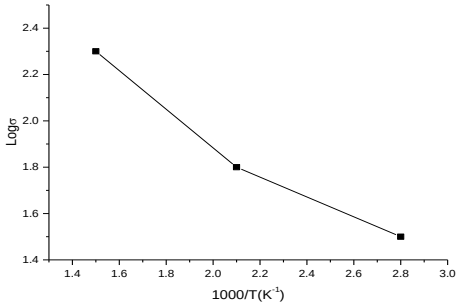

Fig. 11. Variation of electrical conductivity as a function of annealing temperature

5. Conclusions

The effect of thermal annealing on the properties of PbS/CdO core-shell thin film has been investigated. The structural optical and electrical properties of the films were observed to be temperature dependent. The results show that post deposition annealing lowers band gap of the film samples. The optical characteristics of the film samples are suitable for various solar architecture.

Acknowledgement

The authors wish to acknowledge and appreciate the kind assistance from the Biotechnology and Research Development Centre, Ebonyi State University, Abakaliki for giving us access to the facilities in their laboratory for the deposition of the films. This appreciation is extended to the management of the Federal University Ndufu Alike Ikwo for regular payment of salary which facilitated the completion of the work.

References

[1] A. S. Sambo, Energy Sector and Sustainable Development in Nigeria: Issues and Prospects, Lecture delivered at the College auditorium, National Defence College of Nigeria, Abuja, 10th November, 2011.
[2] P. E. Agbo, M. N. Nnabuchi, , Chalcogenide Letters **8**(4), 273 (2011).
[3] P. E. Agbo, Advances in Applied Research **2**(6), 393 (2011).
[4] D. U. Onah, C. E. Okeke, F. I. Ezema, Asian Transactions on Science and Technology **2**(1), 32 (2012).
[5] D. U. Onah, E. I. Ugwu, J. E. Ekpe, American Journal of Nano Research and Applications, **3**(3), 62 (2015).
[6] M. Kavitha, M. Saroja, V. K. Romesh, G. Jenifer, International Journal of Thin Films Science and Technology **5**(2), 137 (2016).
[7] P. E. Agbo, M. N. Nnabuchi, D. U. Onah, Journal of Ovonic Research **7**(2), 29 (2011).
[8] P. E. Agbo, G. F. Ibeh, S. O. Okeke, J. E. Epke, Communications in Applied Sciences **1**(1), 38 (2013).
[9] C. Ariana, ZnO/PbS quantum dot heterojunction photovoltaics, M. Sc Thesis, Universitat De Barcelona, 3-11 (2012)
[10] L. Zhifeng, H. Jianhua, H. Li, G. Keying, L. Yajun, C. Ting, W. Bo, L. Xiaoping, Materials Chemistry and Physics **141**, 804 (2013).
[11] J. Hernández-Borja, Y. V. Vorobiev, R. Ramírez, Sol. Energy Mater. Sol. Cells **95**, 1882 (2011).
[12] P. Derek, Z. Guangmei, J. B. Alison, Z. Daoli, B. A. Glenn, A. C. Sue, Nanomaterials and Nanotechnology **2**, 1 (2012).

[13] V. Maurice, T. Georgelin, J. M. Siaugue, V. Cabuil, J. Magn. Magn. Mater.**321,** 1408 (2009).
[14] M. R. Islam, J. Podder, Cryst. Res. Technol. **44,** 286 (2009).
[15] F. Abeles, Optical Properties of Metals, North- Holland Pub. Co. Amsterdam, 97 (1972).
[16] V. Maurice, T. Georgelin, J.M. Siaugue, V. Cabuil, J. Magn. Magn. Mater. **321,** 1408 (2009).
[17] S. R. Chopra, Thin Film Solar cells. Plenum New York. P.118.1983.
[18] K.S. Chou, C.C. Chen, Mesopor. Mater. **98**, 208 (2007).
[19] Z. Jing, T. Xia, P. Yuan, F. Xiao, J. Zeng, Applied Surface Science **257**, 393-397 (2010).
[20] M. R. Islam, J. Podder, Crystal Research Technology **44** (3), 286 (2009).
[21] B. L. Theraja, Textbook of Electrical Technology; S.C. Hard and Company Ltd, 243 (2007).
[22] A. D. A. Buba, J. S. A. Adelabu, Pacific Journal of Scienec and Technology, **2**(2), 2 (2010).
[23] S. Srikanth, N. Suriyanarayanan, S. Prabahar, V. Balasubramanian, D. Kathirvel, Advances in Science and Research **2**, 95 (2011).
[24] B. Ismail, S. Mushtaq, A. Khan, Chalcogenide Letters **11**(1), 37 (2014).
[25] J. D. Dipalee, S. Shaeed, S. Farha, G. Rrindam, B. Ravikiran, G. G. Anil, S. Ramphai, Advances in Applied Science Research **2**(4), 471 (2011).
[26] C. Augustine, M. N. Nnabuchi, F. N. C. Anyaegbunam, A. N. Nwachukwu, Digest Journal of Nanomaterials and Biostructures **12**(2), 523 (2017).
[27] P. A. Nwofe, P. E. Agbo, Journal of Non-Oxide Glasses **9**(1), 9 (2017).
[28] O. Mustafa, Chin. Phys. Lett 25, 2008.